Hum Genet (2014) 133:625–638
DOI 10.1007/s00439-013-1403-3

ORIGINAL INVESTIGATION

X-linked congenital ptosis and associated intellectual disability, short stature, microcephaly, cleft palate, digital and genital abnormalities define novel Xq25q26 duplication syndrome

R. S. Møller · L. R. Jensen · S. M. Maas · J. Filmus · M. Capurro · C. Hansen · C. L. M. Marcelis · K. Ravn · J. Andrieux · M. Mathieu · M. Kirchhoff · O. K. Rødningen · N. de Leeuw · H. G. Yntema · G. Froyen · J. Vandewalle · K. Ballon · E. Klopocki · S. Joss · J. Tolmie · A. C. Knegt · A. M. Lund · H. Hjalgrim · A. W. Kuss · N. Tommerup · R. Ullmann · A. P. M. de Brouwer · P. Strømme · S. Kjaergaard · Z. Tümer · T. Kleefstra

Received: 8 August 2013 / Accepted: 21 November 2013 / Published online: 11 December 2013

Abstract Submicroscopic duplications along the long arm of the X-chromosome with known phenotypic consequences are relatively rare events. The clinical features resulting from such duplications are various, though they often include intellectual disability, microcephaly, short stature, hypotonia, hypogonadism and feeding difficulties. Female carriers are often phenotypically normal or show a similar but milder phenotype, as in most cases the X-chromosome harbouring the duplication is subject to inactivation. Xq28, which includes *MECP2* is the major locus for submicroscopic X-chromosome duplications, whereas duplications in Xq25 and Xq26 have been reported in only a few cases. Using genome-wide array platforms we identified overlapping interstitial Xq25q26 duplications ranging from 0.2 to 4.76 Mb in eight unrelated families with in total five affected males and seven affected females. All affected males shared a common phenotype with intrauterine- and postnatal growth retardation and feeding difficulties in childhood. Three had microcephaly and two out of five suffered from epilepsy. In addition, three males had a distinct facial appearance with congenital bilateral ptosis and large protruding ears and two of them showed a cleft palate. The affected females had various clinical symptoms similar to that of the males with congenital bilateral ptosis in three families as most remarkable feature. Comparison

R. S. Møller and L. R. Jensen contributed equally to this work.
Z. Tümer and T. Kleefstra contributed equally to this work.

Electronic supplementary material The online version of this article (doi:10.1007/s00439-013-1403-3) contains supplementary material, which is available to authorized users.

R. S. Møller · H. Hjalgrim
Danish Epilepsy Centre, Dianalund, Kolonivej 7, 4293 Dianalund, Denmark
e-mail: rimo@filadelfia.dk

R. S. Møller · C. Hansen · N. Tommerup
Wilhelm Johannsen Centre for Functional Genome Research, Department of Cellular and Molecular Medicine, University of Copenhagen, Copenhagen, Denmark

R. S. Møller · H. Hjalgrim
Institute for Regional Health Services, University of Southern Denmark, Odense, Denmark

L. R. Jensen · A. W. Kuss
Institute for Human Genetics, University Medicine Greifswald, Greifswald, Germany

L. R. Jensen · A. W. Kuss
Interfaculty Institute for Genetics and Functional Genomics, Ernst Moritz Arndt University, Greifswald, Germany

S. M. Maas · A. C. Knegt
Department of Clinical Genetics, Academic Medical Center, Amsterdam, The Netherlands

S. M. Maas
Department of Paediatrics, Academic Medical Center, Amsterdam, The Netherlands

J. Filmus · M. Capurro
Sunnybrook Research Institute, University of Toronto, Toronto, ON, Canada

C. L. M. Marcelis · N. de Leeuw · H. G. Yntema · A. P. M. de Brouwer · T. Kleefstra
Department of Human Genetics, Radboud University Medical Centre, Nijmegen, The Netherlands

K. Ravn · Z. Tümer (✉)
Applied Human Molecular Genetics, Kennedy Center, Copenhagen University Hospital, Rigshospitalet Gl. Landevej 7, 2600 Glostrup, Denmark
e-mail: zeynep.tumer@regionh.dk

of the gene content of the individual duplications with the respective phenotypes suggested three critical regions with candidate genes (*AIFM1, RAB33A, GPC3 and IGSF1*) for the common phenotypes, including candidate loci for congenital bilateral ptosis, small head circumference, short stature, genital and digital defects.

Introduction

Duplications on the long arm of the X-chromosome include intrachromosomal duplications and partial disomies or trisomies resulting from unbalanced translocations with an autosome or Y chromosome. Males with Xq duplications are relatively rare but the increasing use of genome wide molecular cytogenetic studies has identified a growing number of smaller Xq imbalances with a major locus on Xq28 including the *MECP2* gene (Bauters et al. 2008; Lugtenberg et al. 2006; Ramocki et al. 2010; Van Esch et al. 2005; Veltman et al. 2004). Sanlaville et al. (2009) compared three groups of males with Xq duplications: distal (Xq26.3-qter), proximal (Xq21-q24) and *MECP2* duplications only and concluded that they all share common, non-specific, clinical features including intellectual disability (ID), hypotonia, hypogonadism and feeding difficulties. This overlap in phenotype despite discordant Xq duplications was also postulated in a previous study (Cheng et al. 2005) suggesting that there is a common, rather non-specific phenotype, associated with Xq duplications in general. Usually, females with duplications on the X-chromosome are phenotypically normal, as in most cases the duplicated region is subjected to inactivation. However, in females with Xq duplications ID and various other features have been reported (Armstrong et al. 2003; Aughton et al. 1993; Garcia-Heras et al. 1997; Ricks et al. 2010; Sanlaville et al. 2005; Stankiewicz et al. 2005; Tachdjian et al. 2004). The prevalence of duplications comprising more proximal regions of Xq is yet unknown and duplications of Xq25 and Xq26 have been reported in only a few cases (Armstrong et al. 2003; Bauters et al. 2005; Garcia-Heras et al. 1997; Madrigal et al. 2010; Ricks et al. 2010; Schroer et al. 2012; Stankiewicz et al. 2005; Tachdjian et al. 2004). These involve larger duplications, described mainly by conventional cytogenetic studies or microsatellite marker analyses. In this study we report the clinical and molecular characterization of eight unrelated families with interstitial microduplications involving Xq25q26.

Patients and methods

Patients

Eight families were identified through systematic screening for submicroscopic chromosomal imbalances in patients with cognitive disabilities and/or dysmorphic features. The clinical evaluation consisted of a comprehensive medical history, family history, growth measurements and

J. Andrieux
Institut de Génétique Médicale, Hopital Jeanne de Flandre, CHRU, Lille, France

M. Mathieu
Service de Génétique Clinique, CHU d'Amiens, Amiens, France

M. Kirchhoff · A. M. Lund · S. Kjaergaard
Department of Clinical Genetics, Rigshospitalet, University Hospital of Copenhagen, Copenhagen, Denmark

O. K. Rødningen
Department of Medical Genetics, Oslo University Hospital, Ullevaal, Norway

G. Froyen · J. Vandewalle
Human Genome Laboratory, Department of Human Genetics, VIB Center for the Biology of Disease, KU Leuven, Leuven, Belgium

K. Ballon
Department of Paediatrics, University Hospitals Leuven, Louvain, Belgium

E. Klopocki
Institute for Medical and Human Genetics, Charité Universitätsmedizin Berlin, Berlin, Germany

E. Klopocki
Institute for Human Genetics, University of Würzburg, Würzburg, Germany

S. Joss · J. Tolmie
Ferguson-Smith Department of Clinical Genetics, Yorkhill Hospital, Glasgow, UK

R. Ullmann
Max Planck Institute for Molecular Genetics, Berlin, Germany

A. P. M. de Brouwer
Department of Cognitive Neurosciences, Donders Institute for Brain Cognition and Behaviour, Radboud University, Nijmegen, The Netherlands

P. Strømme
Women and Children's Division, Department of Clinical Neurosciences for Children, University Hospital and University of Oslo, Oslo, Norway

dysmorphology examination. All participants have given written informed consent according to the regulations at their local institutional review boards.

Molecular karyotyping

Family I was examined using Agilent 244k oligonucleotide-based microarray analysis (Agilent Technologies). In family II, SNP array analysis was performed using the Affymetrix 250k SNP array platform according to the standard Affymetrix GeneChip protocol (Affymetrix Inc, Santa Clara, CA, USA). In family III, array CGH in the index patient was performed using the Agilent 44K oligonucleotide-based microarray and further confirmed by a 105k array (Oxford design). This 105k array was also applied to test segregation of the Xq duplications in family members. Family IV was examined using Agilent 400K whole-genome oligonucleotide-based microarray analysis (Agilent Technologies, Santa Clara, CA, USA). In family V, an Agilent 44K oligonucleotide-based microarray was used to detect the duplication. Family VI was examined using Agilent 60K whole-genome oligonucleotide-based microarray analysis (Agilent Technologies, Santa Clara, CA, USA). The duplications in family VII and VIII were identified using an X-chromosome-specific array CGH (Bauters et al. 2005) and Agilent 244K oligonucleotide-based microarray (Agilent Technologies, Santa Clara, CA, USA), respectively. For the interpretation of the array results, the UCSC Human Genome Browser: (Hg19, February 2009) (http://genome.ucsc.edu/) was used. The duplications were confirmed by either fluorescence in situ hybridization (FISH) with bacterial artificial chromosome (BAC) DNA probes, quantitative RT-PCR (qPCR) and/or by multiplex ligation-based probe amplification (MLPA) according to standard protocols.

X-inactivation studies

Inactivation status of the X-chromosomes was determined on DNA from lymphocytes using the androgen receptor gene (*AR*) methylation assay (Allen et al. 1992) in families I–VI and a slightly modified *FMR1* (fragile X-mental retardation) methylation assay (Lee et al. 1994) in families I–IV. The X-inactivation was defined as being skewed if more than 80 % of the investigated cells inactivated the same chromosome.

Quantitative RT-PCR

Total RNA was isolated using the PAXgene Blood RNA System (PreAnalytiX GmbH, Hombrechtikon, CH). The expression levels were measured by qRT-PCR in a LightCycler 480 using LightCycler 480 SYBR Green I Master chemistry (Roche, Applied Science). The data were evaluated using the basic relative quantitation algorithm provided with the LightCycler 480 software. For normalization we used 12 housekeeping genes to dilute out the expression variability of single housekeeping genes.

Next-generation paired-end sequencing

Mate pair libraries were prepared using the Mate Pair Library v2 kit (Illumina, San Diego, CA, USA). Briefly, 10 μg DNA was sheared using a nebulizer. Two- to three kb pair fragments were isolated, end-repaired using a mix of natural and biotinylated dNTPs, blunt-end ligated using circularization ligase and fragmented to 200–400 bp. Biotinylated fragments were isolated and end-repaired and A-overhangs were added to the 3′-ends. Paired-end adapters were ligated to the fragments and the library was amplified by 18 cycles of PCR. Mate pair libraries were subjected to 2 × 36 bases paired-end sequencing on a Genome Analyzer IIx (Illumina, San Diego, CA, USA), following the manufacturer's protocol. Reads were aligned to a reference genome using Bowtie allowing up to two mismatches in the seed region. Reads not aligning uniquely were discarded from further analysis. Genomic sequences flanking breakpoints were extracted from the UCSC Genome Browser. Composite sequences mimicking the duplication were constructed and masked for repetitive sequences using repeatmasker (http://www.repeatmasker.org/cgi-bin/WEBRepeatMasker) to avoid designing primers within repetitive sequences. Primers for PCR were designed using Oligo6 software (Molecular Biology Insights). Primer sequences can be obtained upon request. PCR was performed on genomic DNA from duplication carriers and a normal control as templates. The PCR fragments were separated on agarose gel, and the specific bands in the duplication carrier were excised, purified and sequenced on an ABI 3130XL genetic analyzer (Life Technologies) using BigDye terminator chemistry, essentially as described by the manufacturer. The sequences were aligned to composite sequences using Dialign (http://bibiserv.techfak.uni-bielefeld.de/dialign/submission.html) to identify breakpoints. If sequences did not span a breakpoint, new primer sets were designed until spanning PCR products were obtained. Some PCR products were cloned using TOPO TA cloning (Life technologies). Breakpoints were verified by second independent primer-sets.

Gpc3 transgenic mice

We made use of an already generated transgenic mouse model to study effects of overexpression of *Gpc3* (Capurro et al. 2005). We measured the weight of these *Gpc3*

transgenic mice where *Gpc3* expression is driven by the β-actin promoter and compared with normal littermates.

Littermates were weighed at birth (NB), and 1, 2, 3, 4 and 5 weeks after birth (W1, W2, W3, W4 and W5, respectively). For statistical analysis we used the student *t* test.

Results

Extent and size of the Xq25q26 duplications

Using various genome-wide array platforms, we identified overlapping interstitial Xq25q26 duplications ranging from 0.2 to 4.76 Mb in size in eight unrelated families (Fig. 1). None of the index patients showed other pathogenic copy number variations or microscopically visible chromosome rearrangements with conventional cytogenetic analysis. In families I–VI, the duplication was associated with a recognisable phenotype in five males and seven females, whereas the duplication in families VII and VIII was evaluated as a non-pathogenic variation as it was also present in unaffected males. Families I–IV and VI–VIII were Caucasian and family V Pakistani.

Family I comprised three affected individuals, i.e. a mother and her two sons (Fig. 2a–f). 244K oligonucleotide-based microarray analysis revealed a 1.7-Mb interstitial

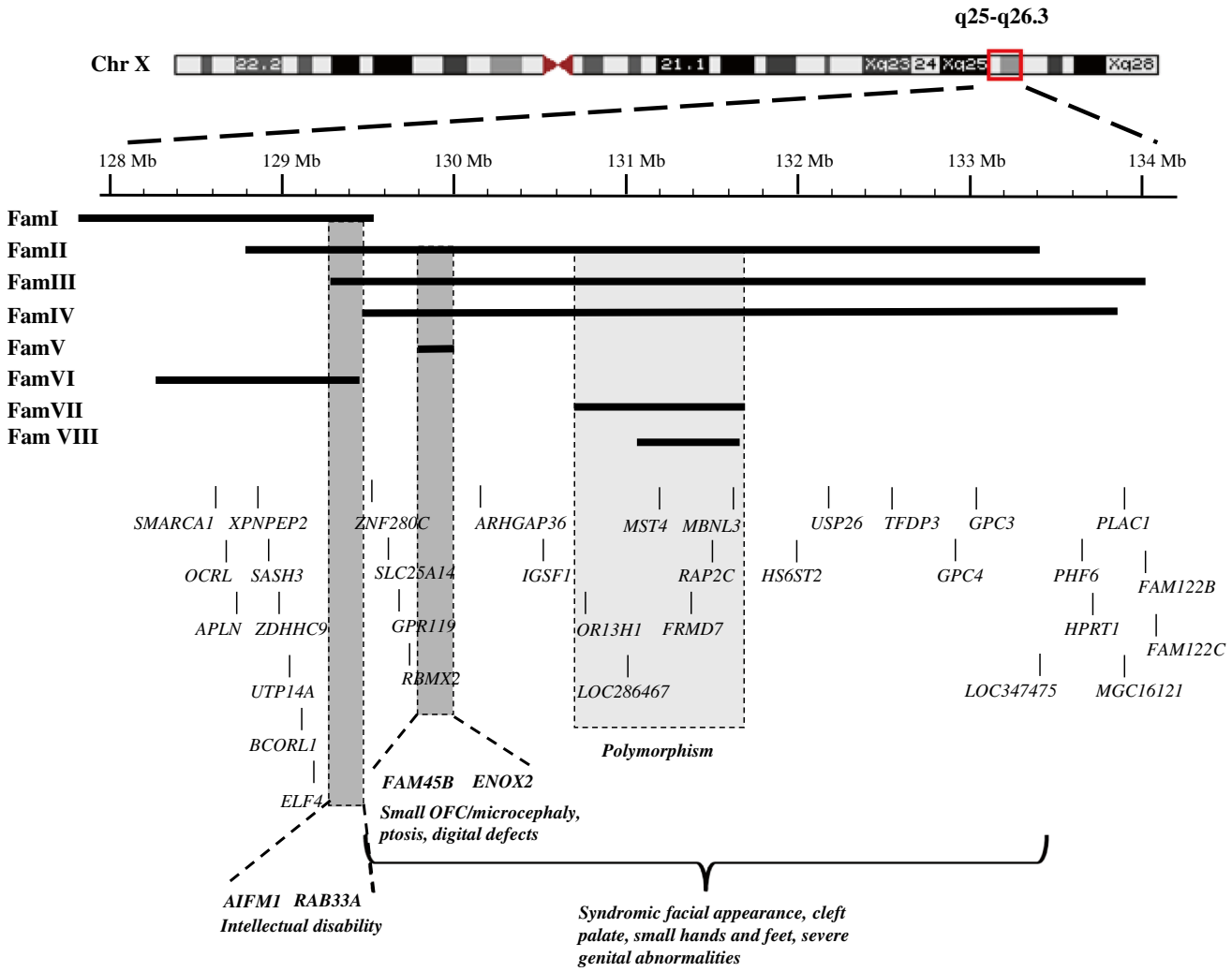

Fig. 1 Schematic representation of the Xq25q26.2 region, including the genes within this interval. The sizes and positions of the duplications found in the eight families are represented by *horizontal bars*. The *left vertical box* highlights the smallest region of overlap (SRO) for the intellectual disabilities observed in families I–III and VI. The region contains two genes, *AIFM1* and *RAB33A*. The *middle vertical box* highlights the SRO for bilateral ptosis, microcephaly and digital defects present in families II–V. This region contains *FAM45B* and *ENOX2*. The *horizontal bracket* shows the SRO for syndromic facial appearance, cleft palate, small hands and feet and severe genital abnormalities. The *right vertical box* highlights the 0.9 Mb polymorphic region, which can be excluded to be disease causing as the duplication of this region has been observed in the unaffected males in families VII and VIII

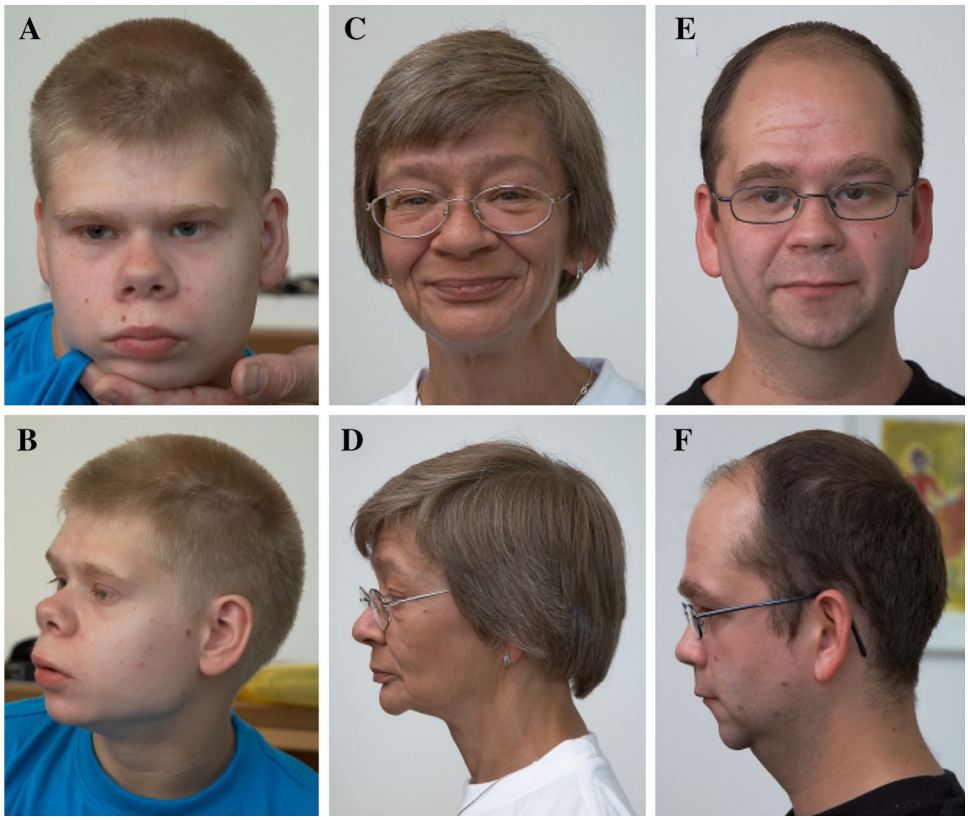

Fig. 2 Facial features of affected individuals of Family I with microduplication of Xq25q26.1. **a**–**e** Affected members of family I. Proband (**a**, **b**), mother (**c**, **d**), brother (**e**, **f**). Note various dysmorphisms including broad nasal tip with thickened alae nasi, anteverted nostrils and long flat philtrum

duplication at chromosome position X: 127, 779, 069–129, 388, 972 (the first and the last aberrant oligonucleotides are A_16_P03766957 and A_16_P21589318, respectively). The duplication was confirmed by FISH and appeared to be in tandem (results not shown). Array CGH revealed the same duplication in the affected mother and the affected brother.

Family II comprised two affected individuals, i.e. a mother and son (Fig. 3a–c). 250K SNP array revealed a 4.7-Mb duplication at chromosome position X: 128, 692, 319–133, 372, 334 (first and last aberrant SNPs are SNP_A-4224853 and SNP_A-1837089, respectively) in both. It was verified by MLPA. The phenotypically normal maternal grandmother did not have the duplication and DNA was not available from the phenotypically normal maternal grandfather. However, SNP evaluation suggested that the duplication was de novo occurring on the grandmaternal allele.

Family III comprised two affected individuals, i.e. a male index patient and his mother (Fig. 3d, f). 44K oligonucleotide-based microarray revealed a 4.76-Mb interstitial duplication (the first and the last aberrant oligonucleotides s are A_14_P135020 and A_14_P122873, respectively; chrX: 129, 213, 749–133, 979, 440) in the index patient and in his mother. The result was confirmed with MLPA and FISH (results not shown). The phenotypically normal maternal grandparents showed normal array profiles.

Family IV comprised two affected individuals, i.e. index patient and his mother (Fig. 3g). High-resolution comparative genome hybridization analysis of the index patient showed an interstitial duplication of Xq25q26, which was maternally inherited. A 400-K whole-genome oligonucleotide microarray was used to fine map the duplication to chrX: 129, 321, 169–133, 860, 490 (4.54 Mb; the first and the last aberrant oligonucleotides are A_16_P03768999 and A_16_P21599361, respectively).

Family V comprised one affected girl (Fig. 2h). 44K oligonucleotide-based microarray analysis revealed a 207-kb interstitial duplication at chromosome position chrX: 129, 630, 006–129, 837, 225 (the first and the last aberrant oligos are A_14_P115358 and A_14_P130575, respectively). The duplication was inherited from the phenotypically normal mother.

Family VI comprised two affected females. Oligonucleotide-based microarray analysis 60K oligo-array) revealed a 985-kb interstitial duplication of Xq25q26.1 at chromosome position chrX: 128, 321, 815–129, 307, 056 (the first and the last aberrant oligos are A_14_P111254 and A_14_P133293, respectively).

In Family VII and VIII array CGH revealed a 0.9 Mb (chrX: 130, 571, 029–131, 352, 535) and 0.7 Mb (chrX: 130, 841, 139–131, 525, 341) interstitial duplication of Xq26, respectively. Segregation analysis was performed, and both duplications were found in healthy male

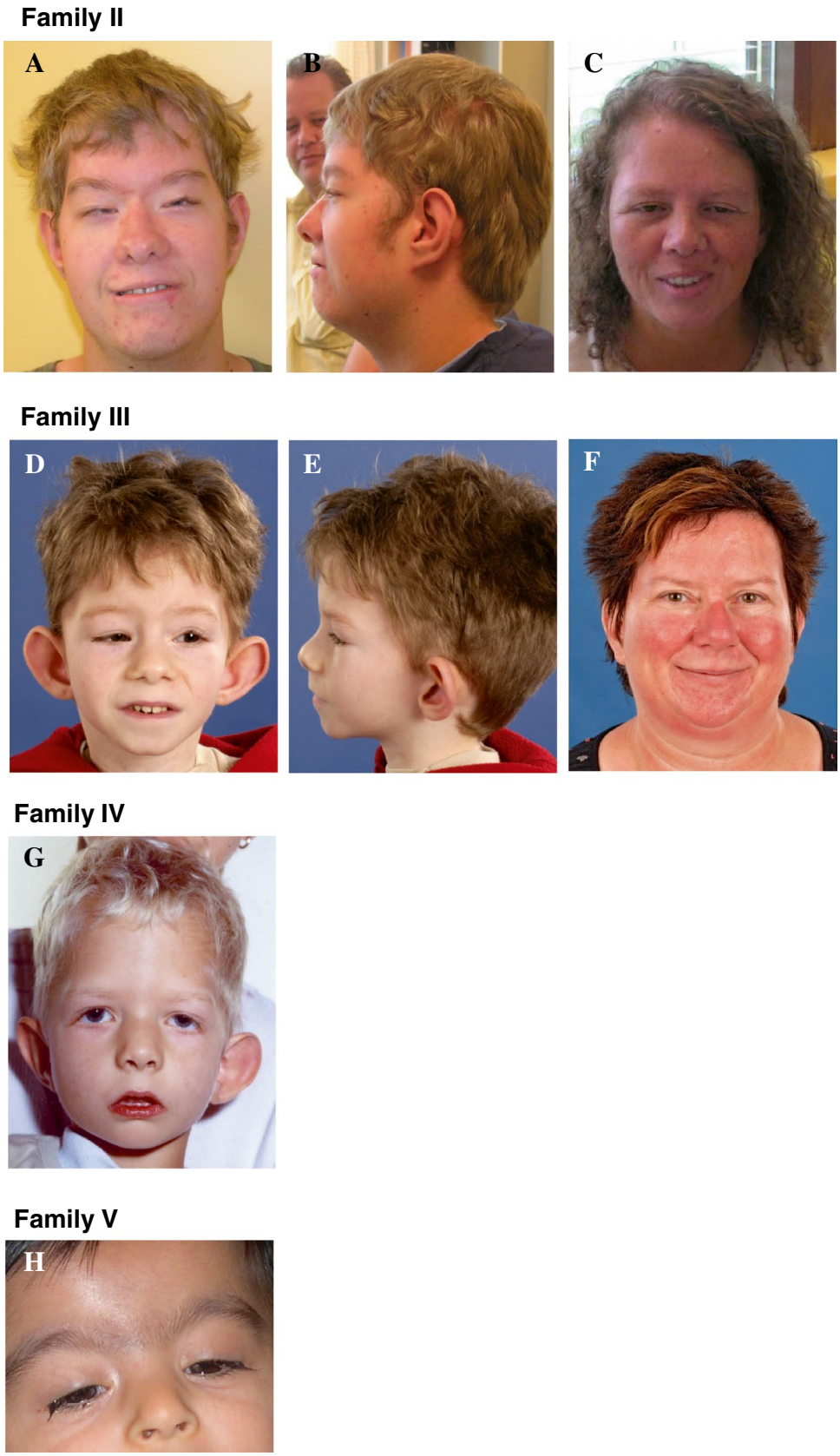

Fig. 3 Facial features of male and female individuals with microduplications of Xq25q26.2. **a–c** Affected members of family II. The proband (**a**, **b**) has bilateral ptosis, telecanthus, blepharophimosis, a broad nasal tip with anteverted nostrils and micrognathia. The mother (**c**) has mild ptosis and anteverted nares. Affected members of family III. The proband (**d**, **e**) has bilateral ptosis, long flat philtrum, thin upper lip and large low set protruding ears. The mother (**f**) was not noted to be dysmorphic. **g** The proband of family IV. Note high forehead, facial asymmetry, large low set protruding ears, down-slanting palpebral fissures, bilateral ptosis, a broad nasal bridge and tip with anteverted nostrils and small mouth with tented upper lip. **h** The proband of family V. Note synophrys, bilateral ptosis, slight epicanthus inversus, and hypermetropia

family members. The observed clinical features in the index patients is most likely related to other, non-genetic causes (supplementary information); however, it cannot be excluded that the duplications may contribute to the ID phenotype.

Clinical evaluations

All five male duplication carriers from family I–IV showed a common phenotype including intrauterine growth retardation and feeding difficulties in childhood (Table 1). They all had various facial dysmorphic signs, comprising a broad nasal tip with thickened alae nasi, bilateral ptosis and large protruding ears (family I–IV) and cleft palate (family II and IV) (Figs. 2, 3). Furthermore, the probands of family II, III and IV had digital anomalies, such as arthrogryposis, camptodactyly, syndactyly, clinodactyly (Supplementary Fig. I) and genital abnormalities, such as hypospadia and a small penis and testes. The male probands in all families, except for family IV, had ID, small head circumference/microcephaly and short stature. All the female duplication carriers showed similar, but milder features including normal cognitive development, except for the mother in family I and the females in family VI, who had borderline ID (Table 2). All the females had short stature and small hands and feet. In families II–V, the carrier females had digital defects; in families II, IV and V bilateral ptosis; and in family VI facioscapulohumeral dystrophy (Figs. 2, 3 and Supplementary Fig. I).

X-inactivation studies

Inactivation status of the X-chromosomes in carrier females was determined on DNA from lymphocytes using the *AR* methylation assay in families I–VI and a slightly modified *FMR1* methylation assay in families I–IV. In the female duplication carriers from families II–IV the X-chromosome harbouring the duplication was preferentially inactivated both for the *AR* and *FMR1* loci (100:0) (supplementary Table 1). In the female duplication carrier in family I the normal X-chromosome was preferentially inactivated (4:96). The mother and the affected daughter in family V showed random X-inactivation in lymphocytes. The females in family VI showed complete skewing of X-inactivation.

mRNA expression studies

The affected males from family I, II and III share a 107-kb region of overlap, which includes two genes, *AIFM1* and *RAB33A*. To investigate the transcriptional level of *RAB33A* and *AIFM1* we obtained blood from the three affected and two unaffected individuals (healthy brother and father of the index patient) of family I. The expression levels were measured by qRT-PCR. The expression values were normalized against that of the unaffected father, which was set to 1 for each of the duplicated genes. Both *RAB33A* and *AIFM* showed higher expression in the affected brothers compared with the mother and the unaffected males from the family. In addition, we performed qRT-PCR on different human brain tissues showing that both *RAB33A* and *AIFMI* are highly expressed in the brain (data not shown), suggesting that dysregulation of *RAB33A* and *AIFMI* may be related to the ID observed in family I and in the other patients.

The affected males and females from families II, III and IV and the female from family V exhibit bilateral ptosis, small head circumference/microcephaly and digital defects, suggesting that the 200-kb common duplicated region in these families is critical for these features. The 200-kb region includes only two genes, *ENOX2* and *FAM45B*. We investigated the transcriptional level of *ENOX2* and *FAM45B* in blood lymphocytes from the affected female of family V and from her unaffected parents. However, the mRNA expression level did not differ significantly in the affected female as compared with her unaffected parents and four healthy controls (Supplementary Fig. II).

Fine mapping of chromosomal breakpoints

The duplications examined in this study vary in size and show different proximal and distal breakpoints in all cases. Fine mapping of the duplication breakpoints in family VI was performed using the next-generation paired-end sequencing followed by PCR cloning which provided base pair resolution; proximal breakpoint: chrX: 128, 280, 363 and distal breakpoint: chrX: 129, 319, 480. A five bp (TTTGT) deletion was observed 35 bp downstream of the distal breakpoint. Both breakpoints were placed outside of genes; however, the distal breakpoint was located only approximately 600 bp from the 3′ UTR of *RAB33A*. The results showed that the breakpoints were located in unique sequences with no apparent homology indicating that nonallelic homologous recombination between flanking segmental duplications is unlikely the rearrangement mechanism underlying the duplication in family VI. Next-generation paired-end sequencing was also performed on the duplication in family I. This analysis revealed that the proximal breakpoint is located in a gene-empty region between chromosomal positions chrX: 127, 743, 035 and chrX: 127, 745, 835 (Hg19). The distal breakpoint [between chromosomal positions 129, 387, 398 and 129, 390, 198 (Hg19)] was predicted to truncate *ZNF280C*.

Table 1 Clinical findings in the affected males

	Family I		Family II	Family III	Family IV
	Proband	Brother	Proband	Proband	Proband
Birth weight (g)	2,130 (−3 SD)	2,000 (−3 SD)	1,030 (<−2.5 SD)	1,065 (<−2.5 SD)	1,810
Birth length (cm)	45 (−3 SD)	46 (−2 SD)	36.5 (<−2.5 SD)	NK	49
OFC (cm)	32.2 (−2 SD)	NK	26 (<−2.5 SD)	28 (<−2,5SD)	NK
Feeding difficulties	+	+	+	+	+
Age at report (years)	17	29	15	4 years 3 months/8 years 2 months	13
Current weight (kg)	36 (−3 SD)	57 (−1 SD)	46.4 (+2.5 SD)	8.8 (−2 SD)/14.2 (−2 SD)	44 (+1 SD)
Current height (cm)	146 (−3 SD)	161 (−3 SD)	142.8 (−4 SD)	89 (<−2 SD)/107 (<−2 SD)	150.4 (−0.5 SD)
Current OFC (cm)	49 (−3 SD)	54 (−1 SD)	50 (−3.5 SD)	7 years 3 months: 46 ½ cm (<−2 SD)	52.2 (−1.5 SD)
Intellectual disability/learning disabilities	+	+	+	+	−
Seizures/epilepsy	+	−	−	+	−
Brain abnormalities	Periventricular leukomalacia, atrophic lesion in the right cerebral hemisphere	NA	NA	Atrophic lesion in the right cerebral hemisphere due to an infarct of the arteria cerebri media	NA
Face	Straight eyebrows, prominent orbital ridge	High forehead, heavy eyebrows, synophrys	Synophrys	Small face, high forehead	High forehead, facial asymmetry
Eyes	Deep set	Myopia	Ptosis, telecanthus, blepharophimosis	Ptosis	Down-slanting palpebral fissures, ptosis
Nose	Broad nasal tip/anteverted nostrils, long/flat philtrum	Broad nasal tip/anteverted nostrils, long/flat philtrum	Broad nasal tip/anteverted nostrils, long/flat philtrum	Broad nasal tip, long flat philtrum	Broad nasal bridge and tip, anteverted nostrils
Mouth	Everted lower lips	Slightly everted lower lips, accentuated nasolabial fissures	Small mouth, cleft palate	Thin upper lip	Tented upper lip, cleft palate
Micrognathia/retrognathia	+	+	+	+	+/Robin sequence
Ears	Normal	Large, simple	Large, dysplastic	Low set posteriorly rotated, protruding	Large, dysplastic, low-set, protruding
Small hands and feet	−	−	+	+	+
Digital defects	−	−	+	+	+
Muscle	Low amount of muscle mass	Normal	Hypotonia	Low amount of muscle mass	Hypotrophy
Genitalia	Normal	Normal	Hypospadia, small testes, crytorchism	Hypospadia, small penis, no testes palpable, hypoplasia of scrotum	Glandular hypospadia, hypoplastic scrotum and penis
Other	Autistic behaviour	Premature balding, retrognathia	Thoracic kypho-scoliosis	Bicuspid aortic valve, thoracolumbar scoliosis	

NK not known, *NA* not analyzed

Table 2 Clinical findings in the female carriers

	Family I Mother	Family II Mother	Family III Mother	Family IV Mother	Family V Proband	Family VI Proband
Birth weight (g)	2,100 (−3 SD)	NK	3,500	3,200	1,488 (32 weeks gestational age)	NK
Birth length (cm)	45 (−3 SD)	NK	NK	51	44	NK
OFC (cm)	NK	NK	NK	NK	30	NK
Feeding difficulties	NK	NK	−	+	−	NK
Age at report (years)	51	40	40	37	4	50
Current weight (kg)	32 (−3 SD)	NK	88	56	12.5 (<3 SD)	42
Current height (cm)	152 (−3 SD)	160 (−2 SD)	160 (−2 SD)	159 (−2 SD)	96 (−3 SD)	152 (−3 SD)
Current OFC (cm)	51 (−2 SD)	51.8 (−2 SD)	55 (−1 SD)	53.5	46.5 (<−3 SD)	NK
Intellectual disability/learning disabilities	+	−	−	−	−	+
Face	Low forehead, arched heavy eyebrows, synophrys	Normal	High forehead	Normal	Increased hair growth on the forehead, synophrys	Normal
Eyes	Hypertelorism, myopia	Mild ptosis	Normal	Mild ptosis	Nystagmus, hypermetropia, ptosis, slight epicanthus inversus and blepharophimosis, increased tearing due to multiple tear duct stenoses	Normal
Nose	Broad nasal tip/anteverted nostrils, visible columnella, long/flat philtrum	Anteverted nostrils	Broad nasal tip	Broad nasal tip	Normal	Normal
Mouth	Large mouth, straight upper lip, accentuated nasolabial fissures	Normal	Normal	Normal	Small triangular shaped mouth	Normal
Micro/retrognathia	+	−	−	Mild	−	−
Small hands and feet	−	+	+	+	−	−
Digital defects	−	+	+	+	+	−
Muscle	Low amount of muscle mass	Normal	Normal	Normal	Normal	Facioscapulohumeral dystrophy
Other				Scoliosis		

NK not known

Decipher database search

There are currently 27 duplications in the Decipher database (http://decipher.sanger.ac.uk/) that overlap or partially overlap the interval from position 128,000,000–134,000,000 on chromosome X. Seven of these duplications are >20 Mbp and due to the large size not considered in this study. The remaining 20 duplications are summarized in supplementary Table I.

Gpc3 transgenic mice

Families II, III and IV have an ~4 Mb overlapping region, 0.9 Mb of which can be excluded to be disease causing as the duplication of this region has been observed in the unaffected males in families VII and VIII. The remaining overlapping region includes 13 genes indicating that increased dosage of one or more of these genes might play a role in disease pathogenesis of the tetrad of clinical features. One of these genes is *GPC3* (Glypican 3). Loss-of-function mutations of *GPC3* lead to the Simpson–Golabi–Behmel overgrowth syndrome (SGBS; MIM #312870). SGBS patients show gigantism, macrocephaly, macrognathia, large hands/feet, and advanced bone age, while the three patients with *GPC3* duplications show prenatal growth retardation, small head circumference/microcephaly, micrognathia, small hands/feet and delayed bone age (Fig. 3). GPC3 was shown to be a negative regulator of Hedgehog (Hh) signalling during mammalian development. Because Hh signalling promotes growth during development, it has been proposed that the overgrowth observed in SGBS patients is, at least in part, due to the hyperactivation of the Hh signalling pathway (Capurro et al. 2008). In good agreement with these observations, *Gpc3* null mice also display developmental overgrowth (Chiao et al. 2002; Pilia et al. 1996).

Interestingly, except for some common symptoms like genital and digital defects and palatal abnormalities, Xq25q26 duplication patients present with almost reverse phenotypes. The males of families II–IV share a remarkable common phenotype including reduced growth, a syndromic facial appearance, small hands and feet, severe genital abnormalities and digital malformations Furthermore, the probands of family II and IV had cleft palate and in addition the proband from family II suffered from oral synechiae (Fig. 3).

We, therefore, studied *Gpc3* transgenic mice where Gpc3 expression is driven by the β-actin promoter (Capurro et al. 2005). The transgenic mice are viable and, with the exception of a mild kidney dysplasia, they display normal embryonic morphogenesis. Importantly, however, these mice are significantly smaller than their wild-type littermates (Fig. 4). This result strongly suggests that the duplication of *GPC3* in families II–IV is responsible, at least in part, for the impaired growth of the patients.

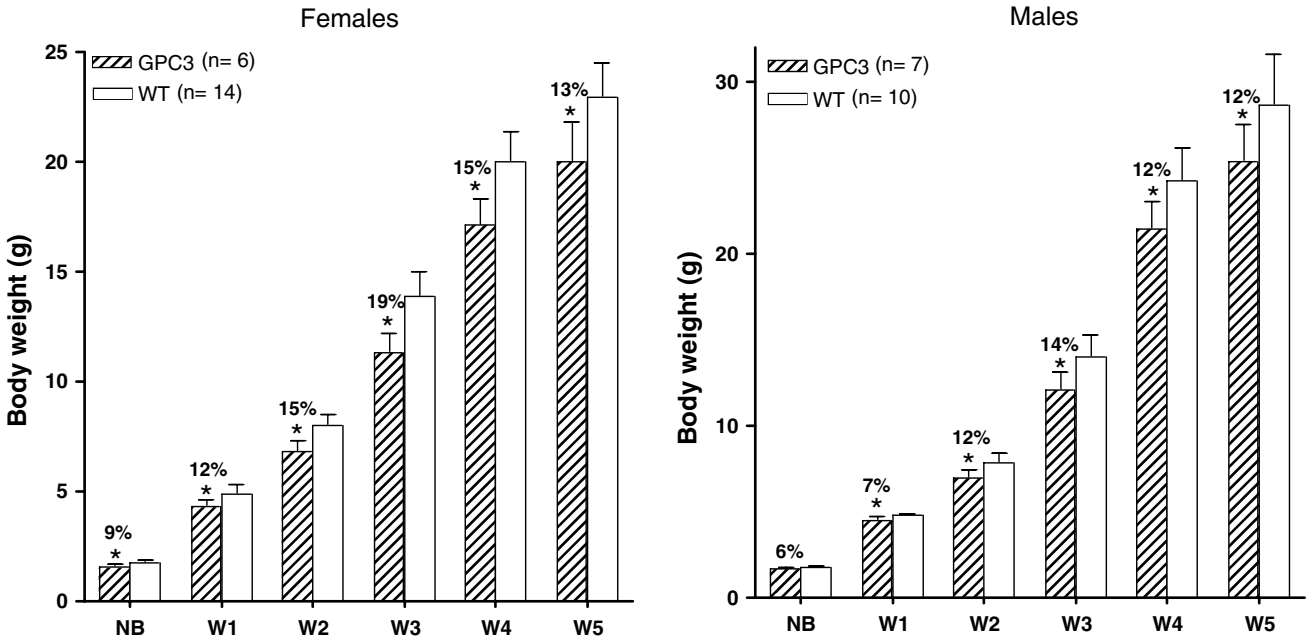

Fig. 4 Weight of Gpc3 transgenic mice and normal littermates. Littermates were weighed at birth (*NB*), and 1, 2, 3, 4 and 5 weeks after birth (W1, W2, W3, W4 and W5, respectively. *$p < 0.05$)

Discussion

We have identified overlapping interstitial Xq25q26 duplications in eight unrelated families. Common features comprise ID, intrauterine- and postnatal growth retardation, feeding difficulties in childhood and small OFC/microcephaly, which are also seen in male patients with microscopically visible Xq duplications. Remarkably, ID was not present in the proband of family IV, who had normal cognitive development and attended normal school. Explanations for this exception may include reduced penetrance, compensatory mechanisms due to different genetic background of this patient, or contribution of genes which are not present in the duplicated region in this proband but shared by the duplicated regions of families I, II and III. As shown in Fig. 1, a 107-kb region of overlap shared by the affected males from family I–III, which includes only the genes *AIFM1* and *RAB33A* fulfils these criteria.

Increased gene dosage of *AIFM1* and *RAB3A* might cause ID

The duplications observed in family I, II, III and VI, which all present an ID phenotype, share a region containing the genes *AIFM1* and *RAB33A*. Schroer et al. (2012) reported on an Xq25 duplication involving six genes (*SMARCA1*, *OCRL*, *APLN*, *XPNPEP2*, *SASH3*, *ZDHHC9* and *UTP14A*) in a patient with autism but without Lowe syndrome features. His mother also carrying the duplication was unaffected. The duplications observed in family I and VI cover this duplication entirely and the family II duplication covers it partially. In line with the observation by Schroer et al. we also did not find features suggesting Lowe syndrome in the families. In family I and VI the female carriers are affected and in family II the mother is mildly affected. It is interesting to speculate that duplication of one or more genes in combination with duplications of *RAB33A* and *AIFM1* could be involved in X-linked ID also affecting female carriers. *AIFM1* encodes the apoptosis-inducing factor (AIF) mitochondrion-associated 1 precursor and *RAB33A* encodes a small GTP-binding protein. We investigated *RAB33A* and *AIFM1* transcriptional levels in lymphocytes from affected and unaffected individuals of family I and V. Fine mapping of the duplication in family VI showed that the distal breakpoint is located approximately 600 bp from the 3′ UTR of *RAB33A*. It is speculative whether this breakpoint leads to deregulation of *RAB33A*. The index patient in family VI had six brothers who all deceased at birth or before the age of 1 year. All of them had severe growth retardation. Haploinsufficiency of *RAB33A* in males has not yet been described, and no truncating mutations of this gene have been observed in the 1,000 Genomes project, Exome Variant Server or dbSNP. The Decipher database lists a few smaller duplications overlapping *RAB33A* and *AIFM1*, but no phenotype is mentioned. However, two duplications of only 293 and 703 kbp (Decipher ID 266609 and 251804) located at Xq26.3 were found in male patients with ID. The two duplications cover the genes *FAM112B* and *FAM122C* as well as the 5′ UTR and coding region of *PLAC1*. Since the duplication in family IV, where no ID was found, covers the *PLAC1* gene but not *FAM122B* or *FAM122C*, it is possible that these two genes contribute to the ID phenotype observed in family II and III. However, *FAM122B* and *C* are functionally uncharacterized genes and future studies are needed to determine the involvement of these genes in brain function.

RAB33A is highly expressed in the brain, especially throughout the cortex and in the hippocampal CA fields (Cheng et al. 2006) and it belongs to the Rab family of small GTPases, and the activity of these GTPases is critical for proper brain function. Mutations in two genes whose protein products affect this pathway; *GDI1* (GDP dissociation inhibitor 1), and *RAB39B* have already been implicated in X-linked ID (D'Adamo et al. 1998; Giannandrea et al. 2010). Increased dosage of *RAB33A* in the brain may also contribute to the intellectual disabilities observed in the present cases as was proposed for duplications and amplifications including the *GDI1* gene at Xq28 (Vandewalle et al. 2009). *AIFM1* encodes the AIF mitochondrion-associated 1 precursor. Mature AIF is a FAD-dependent NADH oxidase targeted to the mitochondrial intermembrane space. Upon apoptogenic stimuli, a soluble form is released by proteolytic cleavage and migrates to the nucleus, where it induces "parthanatos," i.e., caspase-independent fragmentation of chromosomal DNA. Mice with severe reduction in *Aif* expression have progressive degeneration of terminally differentiated cerebellar and retinal neurons (Klein et al. 2002) and *Aif* null embryos fail to increase significantly in size after E9, possibly due to abnormal cell death secondary to reduced mitochondrial respiratory chain complex I activity (Brown et al. 2006). Mutations in *AIFM1* were identified in progressive mitochondrial encephalomyopathy with ID, muscular atrophy and epilepsy (Ghezzi et al. 2010); and in Cowchock syndrome (CMTX4) a slowly progressive X-linked recessive disorder with axonal neuropathy, deafness and cognitive impairment (Rinaldi et al. 2012). It is thus possible that increased dosage of *AIFM1* in critical tissues may contribute to the growth retardation, hypotonia/muscular weakness, epilepsy and the ID observed in the affected members of family I–III and to the facioscapulohumeral dystrophy observed in the females in family VI.

FAM45B and *ENOX2* might play a role in the aetiology of microcephaly, ptosis and digital defects

The affected males and females from families II, III and IV and the female from family V present with bilateral ptosis,

small head circumference/microcephaly and digital defects, suggesting that the 200-kb common duplicated region (Fig. 1) in these families is critical for these features. This region includes only two genes, *ENOX2* and *FAM45B*.

Very little is known about *FAM45B*. It is also not clear whether *FAM45B* is a pseudogene or a non-coding RNA. *ENOX2* (ecto-NOX disulfide-thiol exchanger 2 isoform a) encodes a growth-related cell surface protein. ENOX proteins function as terminal oxidases for plasma membrane electron transport. In addition, they carry out protein disulfide–thiol interchange which is essential to the enlargement phase of cell growth (Morre and Morre 2003). ENOX2 has been suggested to play an essential role in the growth of early embryos (Cho and Morre 2009; Morre and Morre 2003).

In a previous study Xq24q27 region including *FAM45B* and *ENOX2* has been linked to X-linked dominant congenital bilateral isolated ptosis (McMullan et al. 2000), and the present study suggests that duplication of particular sequences in this interval is involved in the development of dominant X-linked congenital ptosis [OMIM 300245]. The mother in family III and in family V was not exhibiting the ptosis. Reduced penetrance was also observed in the original X-linked congenital ptosis family where two females were reported to have the risk-allele but no ptosis. A plausible explanation could be the differences in X-inactivation status in critical tissues. Recently, a female with hemihyperplasia, syndactyly of fingers and toes, bilateral 5th finger clinodactyly, short stature, developmental delay, microcephaly and a 11.2-Mb duplication of Xq25q27.1 was reported (Ricks et al. 2010). Ricks and colleagues suggested a 1.65-Mb critical region including *FAM45B* and *ENOX2* for some of the clinical features including digital anomalies. It is possible that increased dosage of *FAM45B* or *ENOX2* in critical tissues is responsible for the common phenotype including ptosis, small head circumference/microcephaly and digital defects observed in the previously published and in the present cases. A very rare 295-kb duplication (1/2,026) within *ENOX2* has been observed in a single individual by Shaikh et al. (2009). However, this duplication includes only the first three non-coding exons of the gene and to predict its effect is speculative.

mRNA expression analysis

We investigated mRNA expression of the duplicated genes in the two critical regions in blood obtained from individuals of family I and V. We did not observe significant *FAM45B* or *ENOX2* expression differences in the patient from family V, and *RAB33A* expression was only significantly increased in the two affected brothers in family I, when compared with controls and unaffected family members. Though we have not ruled out possible positional effects on other genes in the region, these results suggest that duplications do not necessarily lead to altered mRNA expression, at least in blood. However, the expression profiles of these genes may be different in critical tissues under development, and mRNA expression also depends on other factors such as binding of transcription factors and the epigenetic state of the DNA, both of which are tissue dependent. Furthermore the genetic backgrounds of these families are different and this may have a substantial effect on expression of individual genes.

Glypican 3 and IGSF1 are associated with typical syndromic features

The males of families II, III and IV share a distinct facial appearance with congenital bilateral ptosis and large protruding ears as well as cleft palate in two of them. Furthermore, they all have small hands and feet, obvious genital abnormalities and digital malformations. The critical region for the observed features includes 13 genes suggesting that increased dosage of one or more of these genes might play a role in disease pathogenesis (Fig. 1). The most likely candidate gene in this region is *GPC3* and we show that *Gpc3* transgenic mice are significantly smaller than the wild-type littermates (Fig. 4), indicating that the duplication of *GPC3* in families II–IV is responsible, at least in part, for the impaired growth of the patients. Notably, an intragenic duplication of *GPC3* is described in a Decipher patient (Decipher ID 258050) with the phenotype "large for gestational age" which fits the SGB syndrome phenotype.

The severe genital abnormalities including glandular hypospadia, and hypoplastic scrotum and penis might be caused by the duplication of *IGSF1*, encoding a member of the immunoglobulin-like domain-containing molecule superfamily. This gene is expressed in the developing pituitary primordium and in adult pituitary gland and testis. There are four cases with duplication smaller than 1 Mb covering *IGSF1* in the Decipher database and a phenotype is provided for two cases. In one case (Decipher ID 267829) a male is affected by inguinal hernia, ID, microcephaly and plagiocephaly; and in the other case (Decipher ID 258875) a young boy is affected by blepharophimosis, cleft palate, depressed nasal tip, epicanthus and developmental delay. The latter case is special as his mother received valproate for her seizures, also during pregnancy. His weight at birth was 3.46 kg and he was diagnosed with microcephaly, but at the age of 6 years his head was of average size. He had overlapping toes and received surgery for syndactyly on his right hand. His genitalia, however, were not investigated. He showed severe developmental delay, but an IQ test was not carried out. This case suggests that increased *IGSF1* dosage may be associated with syndromic features, but cannot alone explain all the phenotypic characteristics observed in families II–IV. On the other hand, *IGSF1*

mutations have recently been associated with hypothyroidism and testicular enlargement in males (Sun et al. 2012), suggesting that increased *IGSF1* dosage may contribute to the genital abnormalities observed in families II–IV.

Synopsis

In summary, our study suggests that interstitial duplications of Xq25q26 exhibit a recognisable microduplication syndrome comprising a remarkable facial appearance with congenital bilateral ptosis, cleft palate and large protruding ears, genital and digital defects. Comparison of the duplications and the symptoms suggests several critical regions including a 107-kb region containing *RAB33A* and *AIFM1* for ID and a 200-kb region containing *ENOX2* and *FAM45B* for X-linked congenital ptosis, associated with syn- and clinodactyly. In addition, duplication of *GPC3* might be responsible for the growth impairment in these patients. Identification of additional patients with Xq25q26 duplications will further contribute to the delineation of the clinical spectrum associated with this region.

Electronic database information

Database of Genomic Variants, http://projects.tcag.ca/variation/

Human Genome Browser, February 2009/Hg19, UCSC Human Genome Project http://genome.ucsc.edu/

Decipher database (http://decipher.sanger.ac.uk/)

Acknowledgments We gratefully acknowledge the patients for their invaluable contribution to this study. Wilhelm Johannsen Centre for Functional Genome Research is established by the Danish National Research Foundation. RU was supported by a grant from the German Federal Ministry of Education and Research, NGFNplus, Grant No. PNR-01GS08161.

Conflict of interest None.

References

Allen RC, Zoghbi HY, Moseley AB, Rosenblatt HM, Belmont JW (1992) Methylation of HpaII and HhaI sites near the polymorphic CAG repeat in the human androgen-receptor gene correlates with X-chromosome inactivation. Am J Hum Genet 51:1229–1239

Armstrong L, McGowan-Jordan J, Brierley K, Allanson JE (2003) De novo dup(X) (q22.3q26) in a girl with evidence that functional disomy of X-material is the cause of her abnormal phenotype. Am J Med Genet A 116A:71–76

Aughton DJ, AlSaadi AA, Johnson JA, Transue DJ, Trock GL (1993) Dir dup(X) (q13 ⟶ qter) in a girl with growth retardation, microcephaly, developmental delay, seizures, and minor anomalies. Am J Med Genet 46:159–164

Bauters M, Van EH, Marynen P, Froyen G (2005) X chromosome array-CGH for the identification of novel X-linked mental retardation genes. Eur J Med Genet 48:263–275

Bauters M, Van EH, Friez MJ, Boespflug-Tanguy O, Zenker M, Vianna-Morgante AM, Rosenberg C, Ignatius J, Raynaud M, Hollanders K, Govaerts K, Vandenreijt K, Niel F, Blanc P, Stevenson RE, Fryns JP, Marynen P, Schwartz CE, Froyen G (2008) Nonrecurrent MECP2 duplications mediated by genomic architecture-driven DNA breaks and break-induced replication repair. Genome Res 18:847–858

Brown D, Yu BD, Joza N, Benit P, Meneses J, Firpo M, Rustin P, Penninger JM, Martin GR (2006) Loss of *Aif* function causes cell death in the mouse embryo, but the temporal progression of patterning is normal. Proc Natl Acad Sci USA 103:9918–9923

Capurro MI, Xiang YY, Lobe C, Filmus J (2005) Glypican-3 promotes the growth of hepatocellular carcinoma by stimulating canonical Wnt signaling. Cancer Res 65:6245–6254

Capurro MI, Xu P, Shi W, Li F, Jia A, Filmus J (2008) Glypican-3 inhibits Hedgehog signaling during development by competing with patched for Hedgehog binding. Dev Cell 14:700–711

Cheng SF, Rauen KA, Pinkel D, Albertson DG, Cotter PD (2005) Xq chromosome duplication in males: clinical, cytogenetic and array CGH characterization of a new case and review. Am J Med Genet A 135:308–313

Cheng E, Trombetta SE, Kovacs D, Beech RD, Ariyan S, Reyes-Mugica M, McNiff JM, Narayan D, Kluger HM, Picardo M, Halaban R (2006) Rab33A: characterization, expression, and suppression by epigenetic modification. J Invest Dermatol 126:2257–2271

Chiao E, Fisher P, Crisponi L, Deiana M, Dragatsis I, Schlessinger D, Pilia G, Efstratiadis A (2002) Overgrowth of a mouse model of the Simpson-Golabi–Behmel syndrome is independent of IGF signaling. Dev Biol 243:185–206

Cho N, Morre DJ (2009) Early developmental expression of a normally tumor-associated and drug-inhibited cell surface-located NADH oxidase (ENOX2) in non-cancer cells. Cancer Immunol Immunother 58:547–552

D'Adamo P, Menegon A, Lo NC, Grasso M, Gulisano M, Tamanini F, Bienvenu T, Gedeon AK, Oostra B, Wu SK, Tandon A, Valtorta F, Balch WE, Chelly J, Toniolo D (1998) Mutations in GDI1 are responsible for X-linked non-specific mental retardation. Nat Genet 19:134–139

Garcia-Heras J, Martin JA, Day DW, Scacheri P, Witchel SF (1997) "De novo" duplication Xq23 ⟶ Xq26 of paternal origin in a girl with a mildly affected phenotype. Am J Med Genet 70:404–408

Ghezzi D, Sevrioukova I, Invernizzi F, Lamperti C, Mora M, D'Adamo P, Novara F, Zuffardi O, Uziel G, Zeviani M (2010) Severe X-linked mitochondrial encephalomyopathy associated with a mutation in apoptosis-inducing factor. Am J Hum Genet 86:639–649

Giannandrea M, Bianchi V, Mignogna ML, Sirri A, Carrabino S, D'Elia E, Vecellio M, Russo S, Cogliati F, Larizza L, Ropers HH, Tzschach A, Kalscheuer V, Oehl-Jaschkowitz B, Skinner C, Schwartz CE, Gecz J, Van EH, Raynaud M, Chelly J, de Brouwer AP, Toniolo D, D'Adamo P (2010) Mutations in the small GTPase gene RAB39B are responsible for X-linked mental retardation associated with autism, epilepsy, and macrocephaly. Am J Hum Genet 86:185–195

Klein JA, Longo-Guess CM, Rossmann MP, Seburn KL, Hurd RE, Frankel WN, Bronson RT, Ackerman SL (2002) The harlequin mouse mutation downregulates apoptosis-inducing factor. Nature 419:367–374

Lee ST, McGlennen RC, Litz CE (1994) Clonal determination by the fragile X (FMR1) and phosphoglycerate kinase (PGK) genes in hematological malignancies. Cancer Res 54:5212–5216

Lugtenberg D, de Brouwer AP, Kleefstra T, Oudakker AR, Frints SG, Schrander-Stumpel CT, Fryns JP, Jensen LR, Chelly J, Moraine C, Turner G, Veltman JA, Hamel BC, de Vries BB, van BH, Yntema HG (2006) Chromosomal copy number changes

in patients with non-syndromic X-linked mental retardation detected by array CGH. J Med Genet 43:362–370

Madrigal I, Fernandez-Burriel M, Rodriguez-Revenga L, Cabrera JC, Marti M, Mur A, Mila M (2010) Xq26.2-q26.3 microduplication in two brothers with intellectual disabilities: clinical and molecular characterization. J Hum Genet 55:822–826

McMullan TF, Collins AR, Tyers AG, Robinson DO (2000) A novel X-linked dominant condition: X-linked congenital isolated ptosis. Am J Hum Genet 66:1455–1460

Morre DJ, Morre DM (2003) Cell surface NADH oxidases (ECTO-NOX proteins) with roles in cancer, cellular time-keeping, growth, aging and neurodegenerative diseases. Free Radic Res 37:795–808

Pilia G, Hughes-Benzie RM, MacKenzie A, Baybayan P, Chen EY, Huber R, Neri G, Cao A, Forabosco A, Schlessinger D (1996) Mutations in GPC3, a glypican gene, cause the Simpson–Golabi–Behmel overgrowth syndrome. Nat Genet 12:241–247

Ramocki MB, Tavyev YJ, Peters SU (2010) The MECP2 duplication syndrome. Am J Med Genet A 152A:1079–1088

Ricks CB, Masand R, Fang P, Roney EK, Cheung SW, Scott DA (2010) Delineation of a 1.65 Mb critical region for hemihyperplasia and digital anomalies on Xq25. Am J Med Genet A 152A:453–458

Rinaldi C, Grunseich C, Sevrioukova IF, Schindler A, Horkayne-Szakaly I, Lamperti C, Landoure G, Kennerson ML, Burnett BG, Bonnemann C, Biesecker LG, Ghezzi D, Zeviani M, Fischbeck KH (2012) Cowchock syndrome is associated with a mutation in apoptosis-inducing factor. Am J Hum Genet 91:1095–1102

Sanlaville D, Prieur M, de Blois MC, Genevieve D, Lapierre JM, Ozilou C, Picq M, Gosset P, Morichon-Delvallez N, Munnich A, Cormier-Daire V, Baujat G, Romana S, Vekemans M, Turleau C (2005) Functional disomy of the Xq28 chromosome region. Eur J Hum Genet 13:579–585

Sanlaville D, Schluth-Bolard C, Turleau C (2009) Distal Xq duplication and functional Xq disomy. Orphanet J Rare Dis 4:4

Schroer RJ, Beaudet AL, Shinawi M, Sahoo T, Patel A, Sun Q, Skinner C, Stevenson RE (2012) Duplication of OCRL and adjacent genes associated with autism but not Lowe syndrome. Am J Med Genet A 158A:2602–2605

Shaikh TH, Gai X, Perin JC, Glessner JT, Xie H, Murphy K, O'Hara R, Casalunovo T, Conlin LK, D'Arcy M, Frackelton EC, Geiger EA, Haldeman-Englert C, Imielinski M, Kim CE, Medne L, Annaiah K, Bradfield JP, Dabaghyan E, Eckert A, Onyiah CC, Ostapenko S, Otieno FG, Santa E, Shaner JL, Skraban R, Smith RM, Elia J, Goldmuntz E, Spinner NB, Zackai EH, Chiavacci RM, Grundmeier R, Rappaport EF, Grant SF, White PS, Hakonarson H (2009) High-resolution mapping and analysis of copy number variations in the human genome: a data resource for clinical and research applications. Genome Res 19:1682–1690

Stankiewicz P, Thiele H, Schlicker M, Cseke-Friedrich A, Bartel-Friedrich S, Yatsenko SA, Lupski JR, Hansmann I (2005) Duplication of Xq26.2-q27.1, including SOX3, in a mother and daughter with short stature and dyslalia. Am J Med Genet A 138:11–17

Sun Y, Bak B, Schoenmakers N, van Trotsenburg AS, Oostdijk W, Voshol P, Cambridge E, White JK, le TP, Gharavy SN, Martinez-Barbera JP, Stokvis-Brantsma WH, Vulsma T, Kempers MJ, Persani L, Campi I, Bonomi M, Beck-Peccoz P, Zhu H, Davis TM, Hokken-Koelega AC, Del Blanco DG, Rangasami JJ, Ruivenkamp CA, Laros JF, Kriek M, Kant SG, Bosch CA, Biermasz NR, Appelman-Dijkstra NM, Corssmit EP, Hovens GC, Pereira AM, den Dunnen JT, Wade MG, Breuning MH, Hennekam RC, Chatterjee K, Dattani MT, Wit JM, Bernard DJ (2012) Loss-of-function mutations in IGSF1 cause an X-linked syndrome of central hypothyroidism and testicular enlargement. Nat Genet 44:1375–1381

Tachdjian G, Aboura A, Benkhalifa M, Creveaux I, Foix-Helias L, Gadisseux JF, Boespflug-Tanguy O, Mohammed M, Labrune P (2004) De novo interstitial direct duplication of Xq21.1q25 associated with skewed X-inactivation pattern. Am J Med Genet A 131:273–280

Van EH, Bauters M, Ignatius J, Jansen M, Raynaud M, Hollanders K, Lugtenberg D, Bienvenu T, Jensen LR, Gecz J, Moraine C, Marynen P, Fryns JP, Froyen G (2005) Duplication of the MECP2 region is a frequent cause of severe mental retardation and progressive neurological symptoms in males. Am J Hum Genet 77:442–453

Vandewalle J, Van EH, Govaerts K, Verbeeck J, Zweier C, Madrigal I, Mila M, Pijkels E, Fernandez I, Kohlhase J, Spaich C, Rauch A, Fryns JP, Marynen P, Froyen G (2009) Dosage-dependent severity of the phenotype in patients with mental retardation due to a recurrent copy-number gain at Xq28 mediated by an unusual recombination. Am J Hum Genet 85:809–822

Veltman JA, Yntema HG, Lugtenberg D, Arts H, Briault S, Huys EH, Osoegawa K, de JP, Brunner HG, Geurts van KA, van BH, Schoenmakers EF (2004) High resolution profiling of X-chromosomal aberrations by array comparative genomic hybridisation. J Med Genet 41:425–432